ChemPubSoc Europe

DOI: 10.1002/chem.201304942

CHEMISTRY
A European Journal
Full Paper

Luminescent Probes

Multidentate Europium Chelates as Luminoionophores for Anion Recognition: Impact of Ligand Design on Sensitivity and Selectivity, and Applicability to Enzymatic Assays

Michael Schäferling,* Timo Ääritalo, and Tero Soukka[a]

Abstract: The design of photoluminescent molecular probes for the selective recognition of anions is a major challenge for the development of optical chemical sensors. The reversible binding of anions to lanthanide centers is one promising option for the realization of anion sensors, because it leads in some cases to a strong luminescence increase by the replacement of quenching water molecules. Yet, it is an open problem to gain control of the sensitivity and selectivity of the luminescence response. Primarily, the selective detection of (poly)phosphate species such as nucleotides has emerged as a demanding task, because they are involved in many biological processes and enzymatic reactions. We designed a series of pyridyl-based multidentate europium complexes (seven-, six-, and five-dentate) including sensitizing chromophores and studied their luminescence intensity and lifetime responses to different (poly)phosphates (adenosine triphosphate (ATP), adenosine diphosphate (ADP), adenosine monophosphate (AMP), cyclic adenosine monophosphate (cAMP), pyrophosphate, and phosphate anions), and carboxyanions (citrate, malate, oxalacetate, succinate, α-ketoglutarate, pyruvate, oxalate, carbonate). The results reveal that the number of free coordination sites has a significant impact on the sensitivity and selectivity of the response. Because of its reversibility, the lanthanide probes can be applied to monitor the activity of ATP-consuming enzymes such ATPases and apyrases, which is demonstrated by means of the five-dentate complex.

Introduction

Fluorescent probes (fluoroionophores) for the detection of metal ions are indispensable tools in chemical and environmental analysis or in medical research and diagnosis. The identification of heavy-metal ions in environmental samples, the imaging of Ca^{2+} in living cells, or the determination of Na^{+} and K^{+} concentrations in blood are just a few prominent examples. The design of probes that are sensitive to metal ions is relatively simple and straightforward, because these are spherical and differ only in size and charge. A broad variety of selective receptor systems is available that can be combined with appropriate fluorescent or phosphorescent reporter systems. Chelators such as ethylenediaminetetraacetic acid (EDTA) derivatives, 1,2-bis(*o*-aminophenoxy)ethane-*N*,*N*,*N*′,*N*′-tetraacetic acid (BAPTA), crown ethers, aza crown ethers, or cryptands are frequently used as recognition elements for cation-sensitive indicators.[1]

In contrast, the development of fluoroionophores for anion recognition is much more complex. Anions exhibit a huge structural variety and flexibility; their overall charge depends strongly on the pH and high ionic strength can disturb the recognition. Therefore, the design of anion-sensitive probes with sufficient sensitivity and selectivity is a demanding task in analytical sciences and chemical-sensor technology. In particular, probes for the detection of biologically relevant anions such as phosphates, acetate, carbonate, or halides have been the focal point over the past few years.[2] The difficulties that appeared in the design of probes for selective determination of nucleotides are an outstanding example. Numerous approaches have been pursued to achieve probes that can recognize adenosine triphosphate (ATP) or pyrophosphate with sufficient selectivity over other polyphosphate anions.[3] These include fluorophores functionalized with mono-[4,5] or binuclear zinc dipicolylamine (DPA) complexes[6–12] as a recognition element for polyphosphates. Other attempts utilize functionalized polythiophenes,[13,14] pyrenes,[15] or the indicator displacement strategy based on charge-transfer complexes.[16–18] Recently, a luminescent nanoprobe for ATP based on cysteamine-capped quantum dots was designed.[19] Guanosine nucleotides can be detected by fluorescence quenching of naphthyridine-coated nanoparticles.[20]

It has also been shown that sensitized luminescent lanthanide ions[21] such as europium and terbium show a response to different phosphate species.[22,23] In principle, ligand- or metal-centered interactions of anions with lanthanide complexes can be used as a sensing mechanism.[24–26] The latter is based on the exchange of water molecules that are directly coordinated to the metal center. These quench the lanthanide lumines-

[a] *Dr. M. Schäferling, T. Ääritalo, Prof. T. Soukka*
Department of Biochemistry/Biotechnology
University of Turku, Tykistökatu 6A
BioCity 6th floor, 20520 Turku (Finland)
E-mail: michael.schaeferling@utu.fi

Supporting information for this article is available on the WWW under http://dx.doi.org/10.1002/chem.201304942.

cence by means of nonradiative energy transfer to high-frequency OH oscillations.[27,28] The displacement of water ligands by chelating polyphosphate anions is reversible, and the response in luminescence intensity (or lifetime) can be used to monitor the conversion of ATP in enzymatic reactions in real-time.[23,29] However, in these cases, the sensitizing antenna chromophores such as tetracycline or norfloxacin only form weakly bound complexes with the lanthanide ion. Thus, an excess amount of sensitizer usually has to be added, which leads to compounds with undefined structure and a luminescence response that is prone to many interferences, because oxyanions generally have a high affinity toward europium ions. For example, europium tetracycline responds to citrate and related compounds that occur in the citric acid cycle such as malate and oxaloacetate.[30] At least, the results revealed that multidentate polyphosphates are required to induce a significant luminescence response, which can finally even displace the sensitizer, thus leading to a decrease in luminescence. This was also observed with β-diketonate ligands.[31] The group of Parker et al.[32,33] designed a series of seven-dentate cyclen complexes with europium that bear additional antenna chromophores that can recognize phosphate species and other oxyanions such as hydrogen carbonate[34] or citrate[35] in water. They were also modified for intracellular measurements.[36] A similar approach is based on a carboxy–bipyridyl ligand, but it only shows poor selectivity between different polyphosphates.[37]

The aim of our study is to demonstrate that the systematic variation of binding sites of a multidentate ligand can influence the luminescence response of europium complexes to different anions. The change in the number of coordination sites provides a mode of access to control the sensitivity and selectivity of the response to additional anionic ligands, because defined numbers of free binding sites are now available for polydentate anions. Thus, we synthesized a series of non-macrocyclic 7- to 5-dentate sensitizing ligands, which form stable complexes with europium in aqueous solution and have a limited accessibility for larger anions to the metal center. As Eu^{3+} ions possess up to nine binding sites,[38] two to four open binding sides are available, respectively. We used a phenyl–ethynyl–pyridine chromophore as sensitizer[39,40] and evaluated our concept by studying the luminescence changes in the presence of polyphosphates and biologically relevant oxidic anions such as citrate and related compounds of the citric acid cycle. As the ligand-exchange mechanism occurs fast and reversibly, the 5-dentate complex can be used to monitor the ATP conversion by ATPases or apyrase in real time.

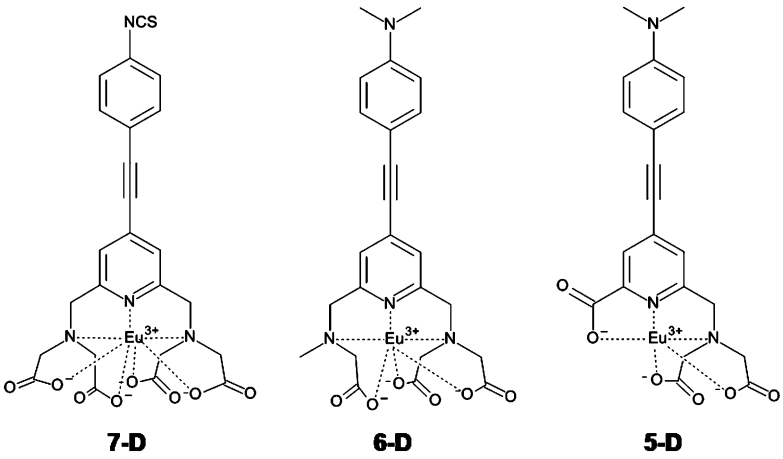

Scheme 1. Chemical structures of the 7-dentate, 6-dentate, and 5-dentate europium complexes.

Results and Discussion

Scheme 1 shows the chemical structures of the studied 7-, 6-, and 5-dentate chelate complexes. Generally, we used the hypersensitive $^5D_0 \rightarrow {}^7F_2$ electronic transition of Eu^{3+}, which displays a maximum at 615 nm, to monitor the luminescence responses. We evaluated the luminescence intensity response to a series of different phosphate species (ATP), adenosine diphosphate (ADP), adenosine monophosphate (AMP), cyclic adenosine monophosphate (cAMP), pyrophosphate (PP_i), and phosphate anions (P_i)) and carboxyanions (citrate, malate, oxalacetate, succinate, α-ketoglutarate, pyruvate, oxalate, carbonate) at pH 7.4 both with a fluorescence spectrometer and a microwell plate reader. As expected, the replacement of water molecules in the first coordination sphere of Eu^{3+} leads to a luminescence increase. The standard deviations of four replicate measurements were generally around 5%.

Synthesis of the 6- and 5-dentate chelate complexes

The synthesis of the europium-7-dentate (**7-D**) complex has been reported previously.[41] The 5-dentate (**5-D**) complex was prepared in five steps starting from 4-bromopyridine-2,6-dicarboxylic acid diethyl ester.[41] This was converted to 4-bromo-6-(bromomethyl)picolinic acid ethyl ester **1** with phosphorus tribromide after selective reduction of one carboxy group with $NaBH_4$. The pyridine triacetate unit **2** was obtained by reaction with diethyl iminodiacetate. Then, the chromophore **3** was formed by coupling the triacetate with 4-ethynyl-*N*,*N*-dimethylaniline. Finally, the carboxylic ester groups were cleaved to yield the 5-dentate ligand **4**, and $EuCl_3$ was added (see Scheme S1 in the Supporting Information).

The synthesis of the 6-dentate (**6-D**) started from 4-bromo-2,6-bis(bromomethyl)pyridine, which was converted with diethyl iminodiacetate to the corresponding diacetate **5**. Then, the second methylbromide unit was reacted with *N*-methylglycine methyl ester to yield the triester **6**. The chromophore **7** was again assembled by coupling with 4-ethynyl-*N*,*N*-dimethylaniline. Scission of all ester groups and transformation to the eu-

ropium complex was performed in one step (Scheme S2 in the Supporting Information).

General properties of the europium chelates

The luminescence properties of the europium chelates are summarized in Table 1. The emission spectra are dominated by the $^5D_0 \rightarrow {}^7F_1$ and $^5D_0 \rightarrow {}^7F_2$ transitions, which peak at 593 and 615 nm, respectively. The luminescence lifetime τ of the $^5D_0 \rightarrow {}^7F_2$ transition of **7-D** in aqueous solution is around 380 μs.[40] The number of water molecules $q(H_2O)$ that are directly coordinated to europium is calculated on the basis of the difference of the luminescence lifetimes (τ) in H_2O and D_2O, according to the equation derived by Supkowski and Horrocks ($q(H_2O) = 1.11[\tau^{-1}(H_2O) - \tau^{-1}(D_2O) - 0.31]$).[42] Correspondingly, it can be deduced that the free binding sites at the europium center in **7-D**, **6-D**, and **5-D** are occupied by two to four water molecules, respectively. Alternative equations for $q(H_2O)$ have been derived from experimental data in the literature by considering the contributions of different oscillators or the quenching effect of unbound water molecules,[42,43] although we reference this simple form of the Horrocks equation. By applying the equation presented by Beeby et al.,[43] the number of coordinated water molecules would be 2.2 for **7-D**,[44] 3.3 for **6-D**, and 4.2 for **5-D**.

Table 1. Spectral properties of the europium chelates.

Europium chelate	7-D	6-D	5-D
Absorbance maximum [nm]	330	355	355
Relative luminescence intensity[a,b] (H_2O)	1	0.0019	0.0006
Luminescence lifetime[a] (H_2O) [μs]	378 ± 0.5[40]	260 ± 50	246 ± 45
Luminescence lifetime[a] (D_2O) [μs]	2017 ± 4[40]	1040 ± 250	2045 ± 310
$q(H_2O)$[c]	2.0	2.9 ± 0.6	3.7 ± 0.7

[a] 615 nm emission, 345 nm excitation. [b] Referenced to **7-D**. [c] According to Horrocks' equation.[42]

The quantum yield of **7-D** chelate was reported to be 0.06.[44] The additional ligation of water molecules causes a more than 500-fold quenching of the luminescence of **6-D** and a more than 1600-fold quenching of **5-D** relative to **7-D**. However, the smaller extinction coefficients of **5-D** and **6-D** can also contribute to the luminescence decrease (see the Supporting Information). The supplementary water ligands cause a significant decrease in the luminescence lifetime in water. The measurements in D_2O indicate that the 5-dentate ligand with the carboxylic acid directly attached to the pyridine ring might cause a closer coordination of the europium to the antenna chromophore, thus leading to a more efficient energy transfer. The bathochromic shifts of the absorption maxima of **5-D** and **6-D** are due to the introduction of the amino substituent. The concentration of the europium chelates was 50 μmol L^{-1} in all measurements.

The conditional stability constants of the complexes were calculated according to a method introduced by Wu and Horrocks.[45] The decrease of luminescence emission was thus measured after the addition of excess amounts of EDTA. The resulting plot for **7-D** is shown by way of example in the Supporting Information (Figure S1). The stability constants K_L have been calculated in analogy to previously described studies[45,46] according to the Equation (1):

$$K_L = K_{EDTA} \frac{[Eu(EDTA)][L]}{[EDTA][EuL]} \quad (1)$$

with:

$$EuL + EDTA \leftrightarrow Eu(EDTA) + L$$

in which L = sum of different protonated free ligands, and K_{EDTA} = conditional stability constant for Eu(EDTA). [EuL] was determined from the fluorescence decrease after the addition of EDTA, and with the assumption that $[EDTA] = [EDTA]_0$ (initial EDTA concentration) and $[Eu(EDTA)] = [L] = [EuL]_0 - [EuL]$, and $\log K_{EDTA} = 14.53$,[44] we calculated the conditional stability constants of the europium chelates to $\log K_L = 19.8 \pm 0.4$ (**7-D**), 16.6 ± 0.3 (**6-D**), and 15.7 ± 0.2 (**5-D**), respectively. For comparison, for the macrocyclic 7-dentate [Eu(do3a)] (H_3do3a = 1,4,7,10-tetraazacyclododecane-1,4,7-triacetic acid) complex $\log K$ values of around 21 have been reported.[45]

All spectral and luminescence intensity response measurements were carried out in a time-resolved (gated) mode with delay times and signal integration times of 400 μs, respectively. Accordingly, it is possible to further optimize the performance of each chelate by tuning the time gates.

Lifetimes of **7-D** were determined by frequency domain measurements.

The 7-dentate complex

Although **7-D** offers two free binding sites that are saturated by water molecules, no response of its luminescence could be observed in the presence of different anions at pH 7.4 over a broad concentration range, neither to phosphate anions (ATP, ADP, PP_i, and P_i) nor to citrate, which is known to be an excellent chelating agent for lanthanides. Thus, the 7-dentate chelate ligand already efficiently shields the europium center from interactions with anions and no replacement of water molecules takes place. It has to be kept in mind that there is an excessive negative charge at the coordination center, which could also prevent the binding of anions.

The 6-dentate complex

The **6-D** complex has three free binding sites that are occupied by water molecules. After the addition of polyphosphate anions, a significant increase in its luminescence intensity can be observed (Figure 1a). For better comparability, the referenced luminescence intensity change (I/I_0) is displayed as obtained by means of a microwell plate reader. The response is rather unselective; there is no distinction between ATP, ADP,

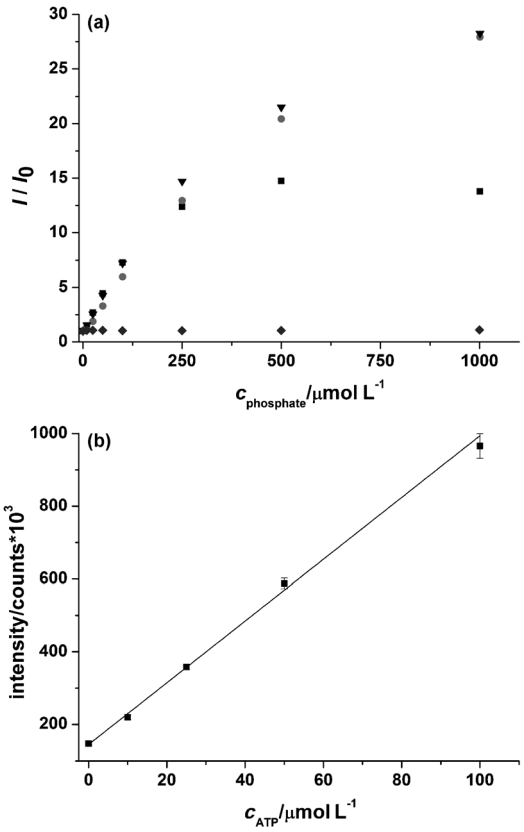

Figure 1. a) Referenced luminescence responses (I/I_0) of **6-D** ($c = 50\ \mu mol\ L^{-1}$) to ATP (■), ADP (●), PP_i (▼), and P_i (◆) in TRIS buffer (pH 7.4). I_0 is the fluorescence intensity in the absence of phosphate; $\lambda_{exc} = 340$ nm, $\lambda_{em} = 615$ nm; time-resolved measurement, delay time: 400 μs, signal integration time: 400 μs. b) Linear range of the ATP response with linear fit (intercept: 145, slope: 8.50, $R^2 = 0.996$) and error bars (SD < 5%).

and P_i in a concentration range from 10 to 250 $\mu mol\ L^{-1}$. At higher concentrations, the response to ATP is saturated, whereas in the case of ADP and PP_i, the increase continues up to concentrations of 1 $\mu mol\ L^{-1}$. In this case, a nearly 30-fold amplification of the luminescence can be achieved. It is clear that the restricted space for binding of voluminous anions provided by the antenna ligand enables no differentiation between anions with two or three phosphate units. Only at a higher excess amount of ADP and PP_i to the chelate (10:1), a difference can be observed relative to the response to ATP. It is probable that a second phosphate molecule can coordinate to europium in the case of the diphosphates if they are present in a high excess amount. The nucleoside rest has no influence on the binding, as there is no difference in the response to ADP and PP_i. Phosphate ions (P_i) have no effect on the luminescence of the chelate. The same is the case for other tested monophosphates such as AMP or cAMP (results not shown). Hence, multidentate polyphosphate anions are required to displace the water molecules from the first coordination sphere, whereas monophosphates do not have this ability. Figure 1b representatively shows the linear range of the response to ATP from 10 to 100 $\mu mol\ L^{-1}$. The limit of detection (LOD) can be calculated from the slope of the linear fit and the standard deviation (3×) of the blank sample and amounts to 20 $\mu mol\ L^{-1}$ for ATP. All luminescence changes were recorded one minute after the addition of the anions.

We also assessed the influence on several carboxyanions such as citrate, malate, oxaloacetate, succinate, α-ketoglutarate, pyruvate, oxalate, and carbonate. Among these, citrate generates a high response with a signal increase of more than 40-fold in the presence of 500 $\mu mol\ L^{-1}$ citrate (Figure 2a),

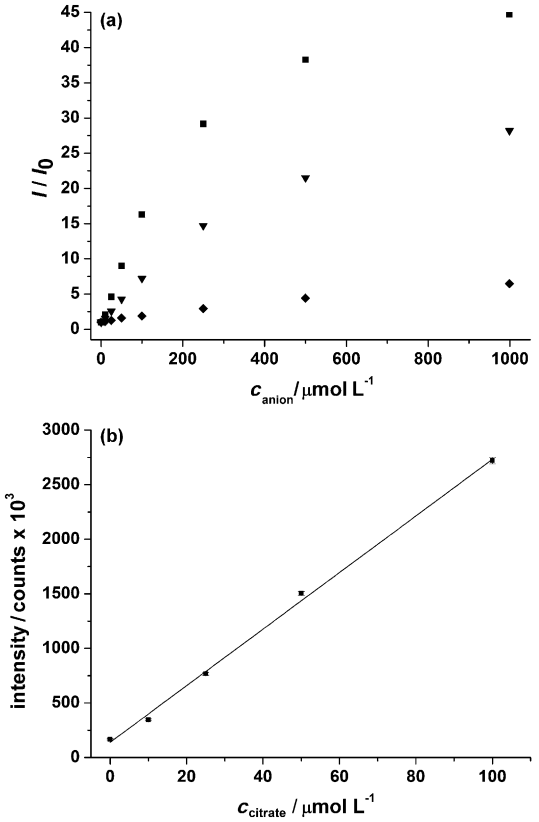

Figure 2. a) Referenced luminescence responses (I/I_0) of **6-D** ($c = 50\ \mu mol\ L^{-1}$) to citrate (■) and oxalate (◆) in TRIS buffer (pH 7.4). I_0 is the fluorescence intensity in the absence of anions. For comparison, the response to PP_i (▼) is also displayed; $\lambda_{exc} = 340$ nm, $\lambda_{em} = 615$ nm; time-resolved measurement, delay time: 400 μs, signal integration time: 400 μs. b) Linear range of the citrate response with linear fit (intercept: 140, slope: 26, $R^2 = 0.992$) and error bars (SD < 5%).

whereas oxalate induces a weak response (six-fold increase). All other tested anions (malate, oxaloacetate, succinate, α-ketoglutarate, pyruvate, carbonate) did not significantly affect the luminescence in this concentration range. The linear range of the citrate detection spans from 10 to 200 $\mu mol\ L^{-1}$ with a LOD around 7 $\mu mol\ L^{-1}$ (Figure 2b). This range can be shifted with the concentration of **6-D**. The results cannot really be compared to other probes for citrate on the basis of europium complexes owing to different emphases and evaluation methods. However, the response seems to be more sensitive than in the case of a cyclen-derived probe.[47] Europium tetracycline provides a lower LOD for citrate determination,[30] but it has only very poor selectivity.

The 5-dentate complex

The additional free binding site at the **5-D** complex results in a dramatic amplification of the response to ATP. A nearly 60-fold increase in the luminescence intensity can be achieved after the addition of 1 mmol L^{-1} of ATP (Figure 3a). This leads

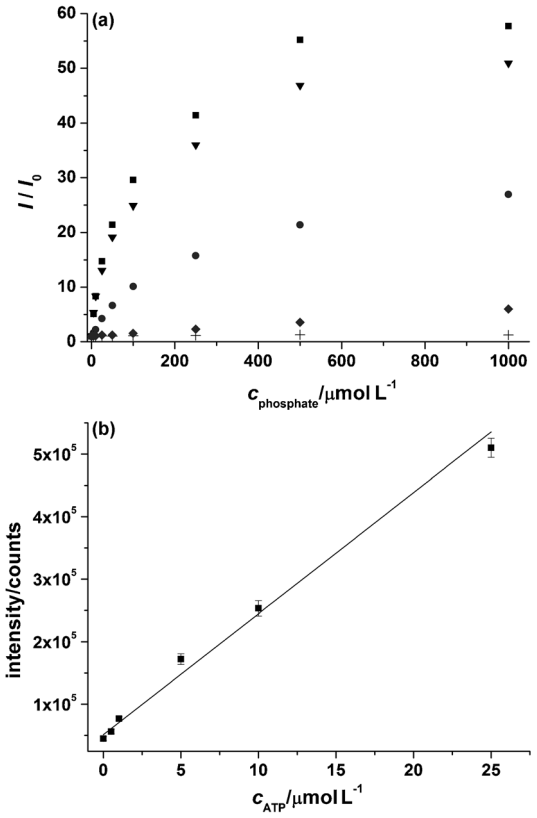

Figure 3. a) Referenced luminescence responses (I/I_0) of **5-D** ($c = 50$ μmol L^{-1}) to ATP (■), ADP (●), AMP (+), PP_i (▼), and P_i (◆) in TRIS buffer (pH 7.4). I_0 is the fluorescence intensity in absence of phosphate; $\lambda_{exc} = 340$ nm, $\lambda_{em} = 615$ nm; time-resolved measurement, delay time: 400 μs, signal integration time: 400 μs. b) Linear range of the ATP response with linear fit (intercept: 51225, slope: 19370, $R^2 = 0.980$) and error bars (SD ≈ 5%).

to an improved sensitivity; the dynamic range of the response to ATP is extended and spans from 0.5 to 500 μmol L^{-1}. Figure 3b shows the corresponding linear range from 0.5 to 25 μmol L^{-1}. The calculated LOD is 0.5 μmol L^{-1} for ATP. Regrettably, the increase in the presence of PP_i is similar. The response to ADP is nearly identical to **6-D**. In both cases a 27-fold rise of the luminescence can be achieved with 1 mmol L^{-1} of ADP. Phosphate ions induce a slight increase (six fold with 1 mmol L^{-1} of P_i), whereas AMP or cAMP (not displayed) did not affect the luminescence. It is evident that the number of phosphate units determines the coordination of the anions to the metal center in **5-D**, and therefore the luminescence response is in the order ATP > ADP > AMP.

However, the bulky nucleoside units have an interfering influence, which can be deduced from the lower increase in the presence of ADP and AMP relative to PP_i and P_i, respectively. This can be confirmed by the comparison of the purine nucleosides ATP/GTP and ADP/GDP, respectively. The guanosines that bear one additional carbonyl group induce a lower luminescence increase than the corresponding adenosine tri- and diphosphates (Figure 4).

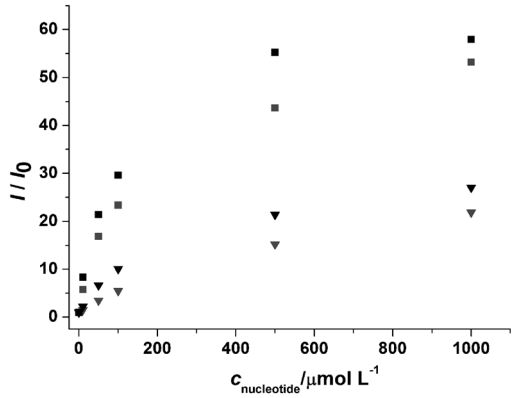

Figure 4. Comparison of the referenced luminescence responses (I/I_0) of **5-D** ($c = 50$ μmol L^{-1}) to ATP(■), ADP(▼), and GTP(■), GDP(▼), respectively. TRIS buffer (pH 7.4); $\lambda_{exc} = 340$ nm, $\lambda_{em} = 615$ nm; time-resolved measurement, delay time: 400 μs, signal integration time: 400 μs.

The signal increase in the presence of citrate is weaker than in the case of **6-D**, which leads to an inversed sensitivity towards ATP (or PP_i) and citrate (Figure 5). A minor reaction to oxalate can also be observed, whereas other carboxyanions (malate, oxaloacetate, succinate, α-ketoglutarate, pyruvate, carbonate) again did not affect the luminescence.

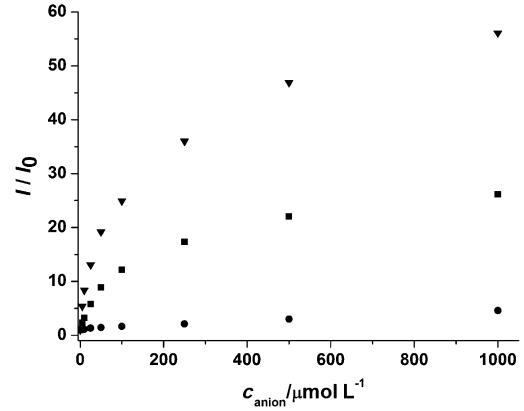

Figure 5. Referenced luminescence responses (I/I_0) of **5-D** ($c = 50$ μmol L^{-1}) to citrate (■) and oxalate (●) in TRIS buffer (pH 7.4). I_0 is the fluorescence intensity in absence of anions. For comparison, the response to PP_i (▼) is also displayed; $\lambda_{exc} = 340$ nm, $\lambda_{em} = 615$ nm; time-resolved measurement, delay time: 400 μs, signal integration time: 400 μs.

Luminescence spectra and lifetimes

The spectral changes of the $^5D_0 \rightarrow {}^7F_1$ ($\lambda_{max} = 593$ and $^5D_0 \rightarrow {}^7F_2$ ($\lambda_{max} = 613/617$ nm) transitions in the presence of ATP are displayed in Figure 6. The emission spectra show intense $^5D_0 \rightarrow {}^7F_2$

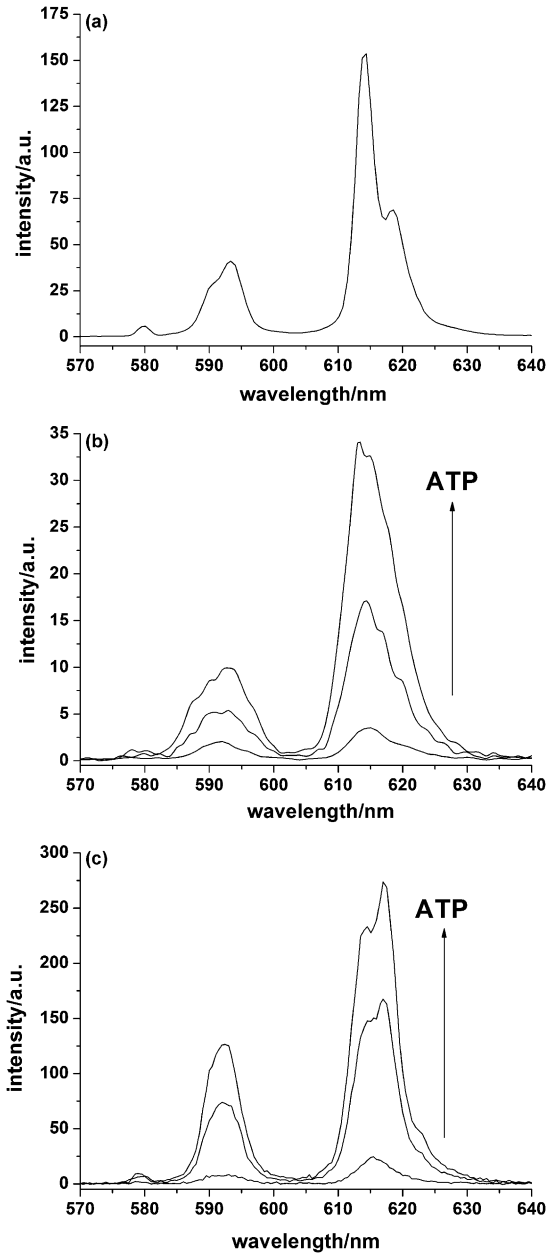

Figure 6. a) Emission spectra of **7-D** ($c = 50\ \mu mol\ L^{-1}$). b) Emission spectra of **6-D** ($c = 50\ \mu mol\ L^{-1}$) in the absence and presence of 10 and 50 $\mu mol\ L^{-1}$ of ATP. c) Emission spectra of **5-D** ($c = 250\ \mu mol\ L^{-1}$) in the absence and presence of 150 and 500 $\mu mol\ L^{-1}$ of ATP; $\lambda_{exc} = 345$ nm; time-resolved measurement, delay time: 400 μs, signal integration time: 400 μs.

transitions with different fine structures after the addition of ATP relative to the reference **7-D**, which reflects the low symmetry of the complexes with ATP. The spectrum of **7-D** shows the typical splitting of the $^5D_0 \rightarrow {}^7F_2$ and $^5D_0 \rightarrow {}^7F_1$ transitions.[44,48,49] However, the three components of the latter could not be completely resolved with the available maximum instrumental resolution (emission slit = 1.5 nm).

The displacement of water molecules from the ligand sphere of europium is accompanied by an increase in the luminescence lifetime. The lifetimes of the $^5D_0 \rightarrow {}^7F_2$ transition of **6-D** and **5-D** in H_2O are indicated in Table 1. The referenced response of the luminescence lifetime (τ/τ_0) of **6-D** to ATP and citrate is shown in Figure 7. In the presence of ATP, the lifetime increases over a dynamic range from 0 to 250 $\mu mol\ L^{-1}$ of ATP from 260 to 675 μs. The results for citrate are similar. In the case of **5-D**, the lifetime increases from 246 to 790 μs in the same concentration range. The lifetimes are determined by means of a time-gated detection of the luminescence intensity after a short pulse of light. Figure S2 in the Supporting Information shows by way of example the resulting decay curves for **5-D** in the absence and presence of 250 $\mu mol\ L^{-1}$ of ATP. The single exponential fits were used to calculate τ. The lifetimes of both complexes exceed the lifetime of the 7-dentate after the addition of ATP. This indicates that only one water molecule remains at the metal center. However, from an analytical perspective, the evaluation of the lifetime responses is less attractive in this case, because the changes are rather small relative to the huge intensity increases, and the measurements were accompanied by high standard deviations up to 20%.

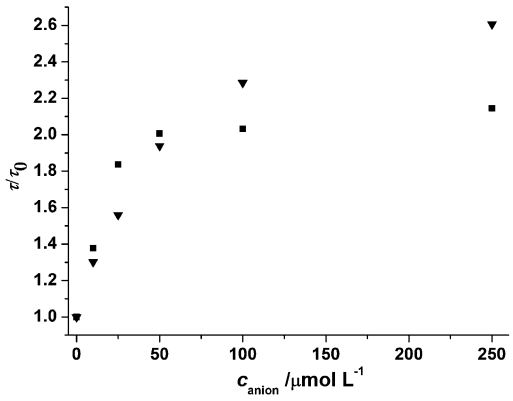

Figure 7. Referenced change of the luminescence lifetime (τ/τ_0) of **6-D** ($c = 50\ \mu mol\ L^{-1}$) to ATP (■) and citrate (▼) in TRIS buffer (pH 7.4); τ_0 is the luminescence lifetime (260 μs) in the absence of anions; $\lambda_{exc} = 340$ nm, $\lambda_{em} = 615$ nm.

Applicability to enzyme assays

We evaluated the reversibility of the response and its applicability to monitor the enzymatic conversion of ATP online by means of two enzymatic assays. Therefore, we used Na^+/K^+-ATPase, which cleaves ATP to ADP and P_i in the presence of Na^+, K^+, and Mg^{2+} ions, and apyrase, which decomposes either ATP or ADP to AMP. First, we studied the influence of ionic strength on the sensitivity of the probe **5-D**. The interference of high salt concentrations on the sensing of anions by luminoionophores turned out to be a fundamental problem. Therefore, we added increasing amounts of NaCl, KCl, and $MgCl_2$ to the 2-amino-2-hydroxymethylpropane-1,3-diol (TRIS) buffer and measured the fluorescence increase after the addition of different concentrations of ATP and ADP. Generally, the ascending slope of the response curve decreases with higher salt concentrations. Figure 8 summarizes the results after the addition of 500 $\mu mol\ L^{-1}$ of the nucleotides. A tremendous attenuation of the luminescence response can be observed in

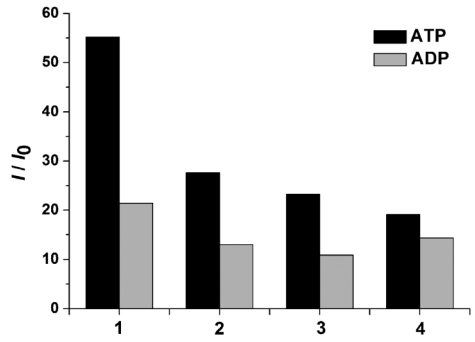

Figure 8. Referenced luminescence increase (I/I_0) of **5-D** ($c = 100\ \mu mol\ L^{-1}$) in the presence of ATP and ADP ($c = 500\ \mu mol\ L^{-1}$) at different ionic strength. 1) TRIS buffer (pH 7.4) without additional salts; 2) Tris + Mg^{2+} (0.5 $\mu mol\ L^{-1}$), K^+ (2.5 $\mu mol\ L^{-1}$), and Na^+ (5 $\mu mol\ L^{-1}$); 3) Tris + Mg^{2+} (2.5 $\mu mol\ L^{-1}$), K^+ (12.5 $\mu mol\ L^{-1}$), and Na^+ (25 $\mu mol\ L^{-1}$); 4) Tris + Mg^{2+} (5 $\mu mol\ L^{-1}$), K^+ (25 $\mu mol\ L^{-1}$), and Na^+ (50 $\mu mol\ L^{-1}$).

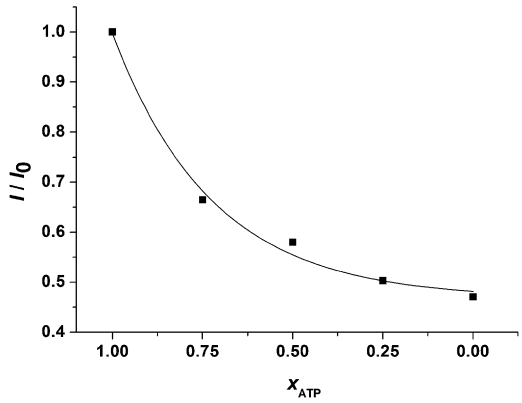

Figure 9. Referenced luminescence intensities (I/I_0) and monoexponential fit of **5-D** ($c = 100\ \mu mol\ L^{-1}$) in TRIS buffer (**2**) in the presence of different mole fractions of ATP, with x(ATP) = [ATP]/([ATP] + [ADP]) and [ADP] = [P_i]. [ATP] + [ADP] = 500 $\mu mol\ L^{-1}$; I_0: intensity for x(ATP) = 1.

the presence of $MgCl_2$ (5 $mmol\ L^{-1}$), KCl (25 $mmol\ L^{-1}$), and NaCl (50 $mmol\ L^{-1}$), which represents optimal salt concentrations for high ATPase activity. The response is predominantly attenuated by the presence of Mg^{2+} ions, which have a high affinity for ATP and shield it from binding to the receptor. This also causes an almost complete loss of the selectivity between ATP and ADP. Nevertheless, after the addition of $MgCl_2$ (0.5 $mmol\ L^{-1}$), KCl (2.5 $mmol\ L^{-1}$), and NaCl (5 $mmol\ L^{-1}$), a sufficiently high response and selectivity between ATP and ADP can be achieved. Thus, we selected these buffer conditions to perform the ATPase assay.

ATPase assay

In the next step, we carried out a calibration of the ATPase reaction [Eq. (2)]:

$$ATP \xrightarrow{ATPase} ADP + P_i \qquad (2)$$

Therefore, we determined the luminescence response in the presence of different molar ratios of ATP and ADP + P_i, assuming an initial concentration of 500 $\mu mol\ L^{-1}$ of ATP (I_0). Figure 9 shows the stepwise decrease in the luminescence of **5-D** with decreasing concentrations of ATP and increasing concentrations of ADP/P_i, until the virtual end point is reached, at which point all ATP is consumed and the concentration of ADP and P_i equals 500 $\mu mol\ L^{-1}$, respectively. In this case, the luminescence drops to approximately 50% of its initial value. The data is fitted monoexponentially according to $y = A_1 \exp(-x/k_1) + y_0$, with $A_1 = 0.01438$, $k_1 = -0.27738$, and $y_0 = 0.4675$ ($R^2 = 0.998$).

The enzymatic assay was performed in the following order. 1) Addition of **5-D** and Na^+/K^+-ATPase to the TRIS buffer that contained Mg^{2+} (0.5 $mmol\ L^{-1}$), K^+ (2.5 $mmol\ L^{-1}$), and Na^+ (5 $mmol\ L^{-1}$). 2) Incubation of the sample mixture for 120 min at 25 °C. 3) Addition of ATP and start of the measurement after 1 min at 25 °C. The final concentration of **5-D** was 100 $\mu mol\ L^{-1}$, and of ATP it was 1 $mmol\ L^{-1}$. For evaluation, the data is plotted from that time when the signal maximum is reached (approximately 4–5 min after addition of ATP).

It is necessary to add the enzyme first and then ATP, because the enzyme also induces a certain increase in the luminescence of the europium chelate, which occurs on a slow timescale. We found out that an incubation time of 120 min is required to ensure a stable initial signal for the measurement after addition of the enzyme before ATP can be added. Figure 10 shows

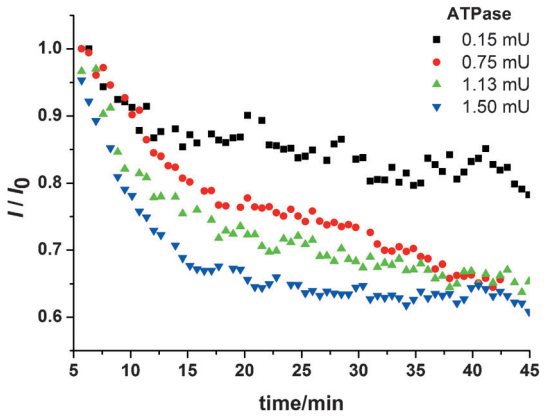

Figure 10. Time traces of the luminescence decrease owing to the conversion of ATP (initial concentration = 1 $mmol\ L^{-1}$) by different concentrations of ATPase from 0.15 to 1.50 mU indicated by **5-D** ($c = 100\ \mu mol\ L^{-1}$). I_0 is the signal maximum after addition of ATP.

the time traces of the conversion of ATP by different amounts of ATPase indicated by the decreasing luminescence of **5-D**. Thus, the turnover of the enzymatic reaction is directly transcribed into a change in the luminescence signal, and the kinetics can be monitored more or less in real time. This is possible because the response to ATP concentrations occurs very fast (within approximately 60 s; Figure S3 in the Supporting Information). The intensities were measured approximately every 30 s. For better comparability, the referenced intensities I/I_0 are displayed, with I_0 as the value of maximal signal after the addition of ATP.

The denoted ATPase activities were determined in the presence of 100 μmol L^{-1} of **5-D** at 25 °C in the selected TRIS buffer by means of a commercially available ATPase assay standard protocol[48] based on the colorimetric Taussky–Shorr reagent (ammonium molybdate/iron(II) sulfate), which indicates the amount of released P_i.[49] It was found that under the assay conditions used here the amount of enzyme required to achieve an activity of 0.06 mU corresponds to an activity of 0.4 mU under optimal conditions (37 °C, Mg^{2+} (5 μmol L^{-1}), K^+ (5 μmol L^{-1}), Na^+ (100 μmol L^{-1})). Thus, the activity is approximately seven times lower than specified by the manufacturer for optimized conditions.

For the first 12 min of the reaction, the data points can be fitted linearly (Figure S4 in the Supporting Information). It can be deduced that the slope of the fit and therefore the initial reaction rate depends linearly on the activity of the added enzyme (Figure S5 in the Supporting Information). The standard errors of the slopes ranged from 3 to 10%. By comparison of the signal drop after 12 min with the calibration function in Figure 9, the amount of consumed ATP can be determined and the resulting enzymatic activity calculated. Table 2 shows the results of the kinetic evaluation using **5-D** and the comparison with the commercially available ATPase assay. Low enzyme activities yielded a comparatively high noise of the recorded time traces, thereby resulting in large deviations in the determined activities relative to the reference method. However, if higher amounts of enzymes are added (≥5 mU), the determined values are in good conformity with the effective activities measured by the Taussky–Shorr reference method.

Table 2. Results of the ATPase assay and comparison with reference method.[48]

Activity of added ATPase[a] [mU]	Measured activity with **5-D**[b] [mU]	Measured initial reaction rate[c] (ΔI) [min]
0.15	0.66	0.018 ± 0.0018
0.75	0.88	0.023 ± 0.0016
1.13	1.25	0.030 ± 0.0028
1.50	1.66	0.035 ± 0.0014

[a] Measured by ATPase assay standard protocol (Taussky–Shorr reagent) under reaction conditions used in this work. [b] According to kinetic analysis. [c] From slopes of linear fits of Figure S1 in the Supporting Information.

For a further assessment of the method, the known inhibitor Ouabain (g-strophanthin) was added to the reaction mixture. Figure S6 in the Supporting Information shows the resulting time traces with 0.75 mU ATPase. The results demonstrate that the probe **5-D** can also indicate the inhibition of ATPases. The enzyme is mostly inhibited in the presence of 1 μmol L^{-1} of Ouabain, whereas 100 μmol L^{-1} completely deactivates the enzyme, which is in accordance with the literature.[50]

Apyrase assay

Apyrases can implement either ATP or ADP as substrate. First we detected the turnover of ATP again by using **5-D** in TRIS buffer as luminescent indicator according to the apyrase reaction [Eq. (3)]:

$$ATP \xrightarrow{apyrase} AMP + 2\,P_i \quad (3)$$

Figure S7 in the Supporting Information shows the time traces of the consumption of ATP by different amounts of apyrase. The enzyme does not interfere with the luminescence of **5-D** in this case. Thus, the order of the addition of the reagents was changed. First, ATP was added and we waited for 30 min until constant signal levels were obtained, then the reaction was started by the addition of the enzyme.

In a second run, we used ADP as substrate, following the reaction [Eq. (4)]:

$$ADP \xrightarrow{apyrase} AMP + P_i \quad (4)$$

We have noticed that high signal differences between ADP and AMP can be achieved in a succinate buffer (results not shown). Again, the ADP was added first, and then, after an incubation time of 30 min, the apyrase. Figure 11 shows the resulting time traces after the addition of different amounts of enzyme. Again, the specified apyrase activities have been determined under the respective assay conditions by using a colorimetric standard procedure.[53]

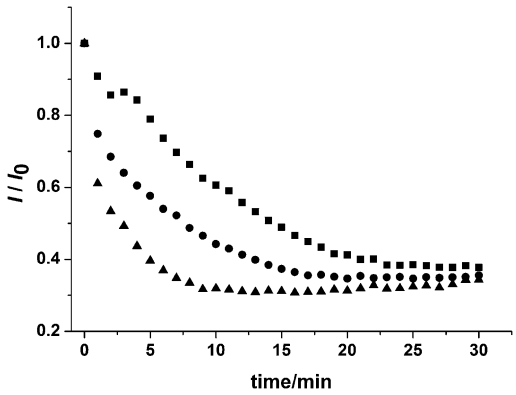

Figure 11. Time traces of the luminescence decrease owing to the conversion of ADP (initial concentration = 0.5 mmol L^{-1}) by different concentrations of apyrase representing 0.036 U (■), 0.072 U (●), and 0.108 U (▲) indicated by **5-D** (c = 50 μmol L^{-1}). I_0 is the signal directly after addition of apyrase (succinate buffer pH 6.6 containing 4 μmol L^{-1} $CaCl_2$).

Conclusion

With this study we have demonstrated that the selectivity and sensitivity of the luminescence response of sensitized europium complexes to anions can be influenced by a variation of the binding sites of the ligand. The number of free coordination sites at the metal center plays an important role in the ability to bind polyphosphates or multidentate oxyanions and to displace water molecules from the ligand sphere of the lanthanide ion.

It has to be noted that the luminescence increase occurs very fast, for **6-D** as well as for **5-D**, and can be monitored after just 1 min reaction time with a saturation after 90 s. The dynamic range of the response can be adjusted with the concentration of the europium complex. The results revealed that **7-D** has no sensitivity to any of the tested anions. Multidentate anions such as polyphosphates or citrate are required for the replacement of water molecules in the cases of **6-D** and **5-D**. The limited space for coordination of bulky anions at the **6-D** center results in a narrow dynamic range of the response to anions and overall a poor selectivity. In contrast, **5-D** exhibits broad dynamic ranges with high sensitivity, particularly for ATP, and a better distinction between different anion species. To summarize, **5-D** appears to be a promising candidate for ATP detection in the absence of PP_i, whereas **6-D** is more suitable as a probe for citrate. These luminoionophores have the typical merits of lanthanide complexes, such as a large wavelength shift between excitation and emission, a sharp emission band, and decay times higher than 100 μs, which are perfectly suited for time-resolved luminescence determination. A displacement of the sensitizing chelate ligand can take place at a high excess amount of anions relative to the europium complex (>25:1), which is indicated by a decrease in luminescence intensities and lifetimes.

As the probe **5-D** shows a fast, reversible, and selective response to ATP (relative to ADP), it can be applied to monitor the conversion of ATP in enzymatic reactions. This has been demonstrated by means of an online ATPase assay. Enzyme activities can be calculated from the recorded luminescence kinetics and the impact of inhibitors can be screened. It is also possible to monitor the conversion of ATP or ADP by apyrases. Although the selectivity between ATP and PP_i is rather low, the differences between the signal responses to ATP, ADP, and AMP are large enough to indicate these enzymatic reactions.

Thus, this probe represents a valuable alternative to commercially available assays for ATPase or apyrase activity, which are all based on end-point methods and require laborious sample-preparation steps. The response characteristic suggests that it can be also used to monitor the activity of kinases or GTPases. The assay protocols can be further optimized by the adaption of temperature, reagents, and salt concentrations, and the type of buffer.

In our future work we aim to further reduce the number of binding sites of the ligand and to evaluate the influence of other factors on the luminescence response such as odd positive charges on the metal center and additional voluminous substituents. The pyridine–diamino–tetraacetic acid structure of the chelating ligand can be easily modified in different ways to achieve a large variety of europium chelates with tailored properties.[54] This could pave the way for the design of luminescent sensors with an improved sensitivity for specific anions. The ligands can be functionalized with amino-reactive groups (e.g., isothiocyanate) as shown in **7-D** and coupled to amino-modified polymer matrices, which can provide an improved selectivity towards different anions and is the basis for the fabrication of ready-to-use optical sensor devices.

Experimental Section

Materials

All reagents were used in American Chemical Society grade. Adenosine 5′-triphosphatase (ATPase) from porcine cerebral cortex, apyrase from potato, and Ouabain octahydrate was obtained from Sigma. Tetrasodium pyrophosphate decahydrate (PP_i) was obtained from Alfa Aesar, sodium hydrogenphosphate dehydrate (P_i) from J.T. Baker, sodium citrate tribasic dehydrate from Riedel-de-Haën; and adenosine-5′-triphosphate disodium salt (ATP), adenosine-5′-diphosphate sodium salt (ADP), adenosine 5′-monophosphate sodium salt (AMP), adenosine-3′,5′-cyclic monophosphate sodium salt (cAMP), adenosine 3′,5′-cyclic monophosphate (cAMP), oxaloacetic acid, sodium pyruvate, α-ketoglutaric acid disodium salt dehydrate, sodium oxalate, L-malic acid, sodium carbonate monohydrate, and succinic acid were obtained from Sigma–Aldrich.

Synthesis of 5-D complexes

4-Bromo-6-(bromomethyl)picolinic acid ethyl ester (1): 4-Bromopyridine-2,6-dicarboxylic acid diethyl ester (7.1 g, 23 mmol) was dissolved in ethanol (70 mL), and granular $NaBH_4$ (770 mg) was added. The mixture was heated at reflux for one hour, and a white precipitate was formed. The solvent was evaporated with a rotary evaporator, and water (70 mL) was added. After stirring at room temperature for 10 min, the product was extracted with CH_2Cl_2 (ca. 100 mL). Purification with column chromatography (10% MeOH/CH_2Cl_2) gave the intermediate (1.2 g). This was dissolved in DMF (6 mL) and the solution was added dropwise to PBr_3 (0.516 mL) in DMF (3 mL). The mixture was stirred at room temperature overnight. After this, 5% $NaHCO_3$ (ca. 10 mL) was added and the solution was extracted with petroleum ether. After evaporation, pure product **1** (1.2 g, 4 mmol) was obtained with short filtration through a silica layer using CH_2Cl_2 as eluent.

Diethyl-2,2′-({[bromo-(6-ethoxycarbonyl)pyridine-2-yl]methyl}-azenediyl)diacetate (2): 4-Bromo-6-(bromomethyl)picolinic acid ethyl ester (1.2 g), diethyliminodiacetate (0.845 mL), and K_2CO_3 (800 mg) were added to acetonitrile (50 mL), and the mixture was heated to reflux. The reaction was followed with TLC (30% petroleum ether/ethyl acetate) and after 4 h, only one compound was visible. The mixture was filtered and the filtrate was evaporated to dryness. After column chromatography using 25% ethyl acetate/petroleum ether (EtOAc/PE) as eluent, pure product **2** (1.5 g, 3.5 mmol) was obtained.

Diethyl 2,2′-{[(4-{[4-(dimethylamino)phenyl]ethynyl}-6-(ethoxycarbonyl)pyridin-2-yl)methyl]azanediyl}diacetate (3): Compound **2** (310 mg, 0.73 mmol) and 4-ethynyl-*N*,*N*-dimethylaniline (120 mg) were dissolved in Et_3N/THF (5 mL/5 mL), and the solution was saturated with argon for 5 min, then $[Pd(PPh_3)Cl_2]$ (7 mg) and CuI (4 mg) were added. The mixture was kept under argon flow for 10 min, then the bottle was capped, and it was stirred for 3 days under an argon atmosphere at 54 °C. The solvents were evaporated, and CH_2Cl_2 (40 mL) was added. The organic phase was washed twice with water (40 mL) and then evaporated to dryness. Purification was carried out with silica gel chromatography by using an EtOAc/PE gradient. The treatment with 15% EtOAc/PE eluted various catalyst parts and the first visible fractions, whereas the last yellow fraction was eluted with 50% EtOAc/PE and gave the pure product **3** (260 mg, 0.52 mmol).

2,2′-{[(6-Carboxy-4-{[4-(dimethylamino)phenyl]ethynyl}pyridin-2-yl)methyl]azanediyl} diacetic acid (4): Compound **3** (50 mg, 100 μmol) was dissolved in methanol (5 mL) and moved to a round bottom flask. Concentrated HCl (5 mL) was added, and the methanol was evaporated. Afterwards, the solution was heated under reflux conditions for 3 h and evaporated to dryness to obtain product **4** (40 mg, 97 μmol).

Synthesis of 5-D: Saponified ligand **4** (25 mg) was dissolved in water (0.5 mL), and the solution was neutralized with $NaHCO_3$. Afterwards, $EuCl_3 \cdot 6H_2O$ (15 mg) dissolved in water (0.1 mL) was added while the solution was kept at neutral pH.

Synthesis of 6-D complexes

Diethyl 2,2′-({[4-bromo-6-(bromomethyl)pyridin-2-yl]methyl}azanediyl)diacetate (5): 4-Bromo-2,6-bis(bromomethyl)pyridine (3 g, 9 mmol) was dissolved in acetonitrile (60 mL) at 50 °C. Potassium carbonate (6 g) and diethyliminodiacetate (1 mL) were added, and the mixture was stirred at 60 °C for 3 h. Then the mixture was filtered, and the filtrate was evaporated to dryness. Purification with column chromatography (20% EtOAc/PE) resulted in product **5** (1.5 g, 3.3 mmol) and unreacted starting material (1.07 g).

Diethyl 2,2′-{[(4-bromo-6-{[(2-methoxy-2-oxoethyl)(methyl)-amino]methyl}pyridin-2-yl)methyl]azanediyl}diacetate (6): Compound **5** (250 mg, 1.75 mmol), K_2CO_3 (100 mg), and *N*-methylglycine methyl ester (400 mg) were dissolved in acetonitrile (10 mL), and the mixture was heated under reflux conditions for 20 h. The mixture was filtered, then the filtrate was evaporated to dryness and purified with column chromatography by using PE as the main solvent and applying an EtOAc gradient from 20 to 50%. Compound **6** (280 mg, 0.60 mmol) was obtained with a 50% gradient.

Diethyl 2,2′-{[(4-{[4-(dimethylamino)phenyl]ethynyl}-6-{[(2-methoxy-2-oxoethyl)(methyl)amino]methyl}pyridin-2-yl)methyl]azanediyl}diacetate (7): Compound **6** (280 mg) and 4-ethynyl-*N*,*N*-dimethylaniline (120 mg) were dissolved in Et_3N/THF (5 mL/5 mL) and the mixture was flushed with argon for 10 min. Then [Pd-$(PPh_3)Cl_2$] (1 mg) and CuI (1 mg) were added, and the mixture was kept under argon flow for another 10 min. After this, the flask was capped and stirred at 54 °C overnight. The solvents were evaporated and the residue dissolved in a small volume of EtOAc. Purification with column chromatography using an EtOAc/PE gradient (10 to 50%) resulted in product **7** (300 mg, 0.56 mmol).

Synthesis of 6-D: Compound **7** (240 mg) was dissolved in methanol (5 mL). Then concentrated HCl (8 mL) was added, and the mixture was heated under reflux conditions for 3 h, then evaporated to dryness. The saponified ligand was dissolved in water (10 mL) and neutralized with $NaHCO_3$. $EuCl_3 \cdot 6H_2O$ (170 mg) was dissolved in water (2 mL) and added. After 2 h at room temperature, the formed precipitate was collected by centrifugation. After drying under reduced pressure, **6-D** (118 mg, 0.19 mmol) was obtained.

Spectroscopy

Spectroscopic characterization of the ligands and europium complexes (UV/Vis, NMR spectroscopy, MS) can be found in the Supporting Information.

For spectroscopic analysis, all measurements were carried out in quartz cuvettes. The concentration of the europium chelates was always 50 μmol L^{-1} in 25 mM TRIS buffer (pH 7.4) if not otherwise stated. The corresponding amounts of anions were subsequently added in the form of highly concentrated solutions in TRIS buffer. Absorption spectra were recorded using a Varian Cary 300 Bio UV/Vis instrument. Luminescence spectra and lifetimes were recorded using a Varian Cary Eclipse fluorescence spectrophotometer. The uncorrected spectra were obtained in the phosphorescence mode with delay and gate times of 400 μs, respectively, at an excitation wavelength of 345 nm and emission slits of 1.5 or 2.5 nm. The lifetime measurements were carried out by integrating 100 excitation cycles with a delay time of 100 μs and a gate time of 40 μs.

Microwell plate assays

The luminescence responses to the anions were measured using a Victor 1420 Multilabel counter from Wallac, Perkin–Elmer Life and Analytical Sciences (Wellesley, MA). The excitation wavelength was 340 nm, and the detection wavelength 615 nm. A time-resolved detection mode was used with a delay time and signal integration time of 400 μs, respectively. All measurements were performed 1 min after addition of the anions in 96-microwell plates with transparent flat bottom from Nunc in four replicates. The final sample volume was 100 μL in each well, which contained the europium chelate (50 μmol L^{-1}) and the corresponding amount of anions in 25 mM TRIS buffer (pH 7.4).

The ATPase assays were carried out by dissolving the required amount of **5-D** and ATPase (+inhibitor) in TRIS buffer that contained Mg^{2+} (0.5 μmol L^{-1}), Na^+ (5 μmol L^{-1}), and K^+ (2.5 μmol L^{-1}) to achieve the desired final concentrations or activities, respectively. The sample mixture was incubated at 25 °C for 2 h. Finally, the necessary amount of an ATP stock solution, which was thermostatted at 25 °C, was added to give a final volume of 100 μL per well and the measurement was started after 1 min. In this case, the final concentrations were 100 μmol L^{-1} of **5-D** and 1 mmol L^{-1} of ATP per well. The mean intensities from three parallel runs are always displayed.

The apyrase assays were performed in a similar way. The succession of reagent addition was in this case **5-D**, ATP or ADP (incubation for 30 min at 25 °C), and finally apyrase. The reaction with ATP as substrate was carried out in 25 mM TRIS buffer (pH 6.6) that contained Ca^{2+} (1 μmol L^{-1}) at 25 °C. The reaction with ADP was carried out in 40 mM succinate buffer (pH 6.6) that contained Ca^{2+} (4 μmol L^{-1}).

The conditional stability constants were determined by the addition of excess amounts of EDTA to the europium chelates in three replicate measurements. The luminescence evaluation was carried out by using **7-D** (1 nmol L^{-1}) and different batches of EDTA between 100 and 500 μmol L^{-1} after a reaction time of 48 h at 50 °C, **6-D** (1 μmol L^{-1}) with EDTA batches between 10 and 100 μmol L^{-1} (48 h, RT), and **5-D** (5 μmol L^{-1}) with EDTA batches between 75 and 200 μmol L^{-1} (48 h, RT).

Acknowledgements

The authors thank Joonas Mäkelä for providing the **7-D** chelate. M.S. acknowledges TEKES (Finnish Funding Agency for Technology and Innovation) for financial support.

Keywords: anions · chelates · lanthanides · luminescence · sensors

[1] M. Schäferling, *Angew. Chem.* **2012**, *124*, 3590 – 3614; *Angew. Chem. Int. Ed.* **2012**, *51*, 3532 – 3554.
[2] T. Gunnlaugsson, M. Glynn, G. M. Tocci, P. E. Kruger, F. M. Pfeffer, *Coord. Chem. Rev.* **2006**, *250*, 3094 – 3117.
[3] C. Spangler, M. Schäferling, O. S. Wolfbeis, *Microchim. Acta* **2008**, *161*, 1 – 39.
[4] S. J. Lee, A. S. Rao, Y. H. Shin, H.-J. Chung, Y. Huh, K. H. Ahn, J. Jung, *J. Mol. Histol.* **2013**, *44*, 241 – 247.
[5] M. Schäferling, T. Lang, A. Schnettelker, *J. Fluoresc.* **2013**, DOI 10.1007s10895 – 013 – 1292 – 9.
[6] C. Park, J.-I. Hong, *Tetrahedron Lett.* **2010**, *51*, 1960 – 1962.
[7] Y. Kurishita, T. Kohira, A. Ojida, I. Hamachi, *J. Am. Chem. Soc.* **2010**, *132*, 13290 – 13299.
[8] A. Ojida, S. K. Park, Y. Mito-oka, I. Hamachi, *Tetrahedron Lett.* **2002**, *43*, 6193 – 6195.
[9] A. Ojida, Y. Miyahara, J. Wongkongkatep, S. Tamaru, K. Sada, I. Hamachi, *Chem. Asian J.* **2006**, *1*, 555 – 563.
[10] Y. J. Jang, E. J. Jun, Y. J. Lee, Y. S. Kim, J. S. Kim, J. Yoon, *J. Org. Chem.* **2005**, *70*, 9603 – 9606.
[11] D. H. Lee, S. Y. Kim, J. I. Hong, *Angew. Chem.* **2004**, *116*, 4881 – 4884; *Angew. Chem. Int. Ed.* **2004**, *43*, 4777 – 4780.
[12] A. J. Moro, J. Schmidt, T. Doussineau, A. Lapresta-Fernandéz, J. Wegener, G. J. Mohr, *Chem. Commun.* **2011**, *47*, 6066 – 6068.
[13] C. Li, M. Numata, M. Takeuchi, S. Shinkai, *Angew. Chem.* **2005**, *117*, 6529 – 6532; *Angew. Chem. Int. Ed.* **2005**, *44*, 6371 – 6374.
[14] C. Spangler, T. Lang, M. Schäferling, *Dyes Pigm.* **2012**, *95*, 194 – 200.
[15] Z. Xu, N. J. Singh, J. Lim, J. Pan, H. N. Kim, S. Park, K. S. Kim, J. Yoon, *J. Am. Chem. Soc.* **2009**, *131*, 15528 – 15533.
[16] S. L. Wiskur, H. Ait-Haddou, J. J. Lavigne, E. V. Anslyn, *Acc. Chem. Res.* **2001**, *34*, 963 – 972.
[17] S. Atilgan, E. U. Akkaya, *Tetrahedron Lett.* **2004**, *45*, 9269 – 9271.
[18] P. P. Neelakandan, M. Hariharan, D. Ramaiah, *J. Am. Chem. Soc.* **2006**, *128*, 11334 – 11335.
[19] W. Tedsana, T. Tuntulani, W. Ngeontae, *Anal. Chim. Acta* **2013**, *783*, 65 – 73.
[20] P. J. M. Cywinski, A. J. Moro, T. Ritschel, N. Hildebrandt, H.-G. Löhmannsröben, *Anal. Bioanal. Chem.* **2011**, *399*, 1215 – 1222.
[21] J.-C. G. Bünzli, *Chem. Rev.* **2010**, *110*, 2729 – 2755.
[22] Y. Miao, J. Liu, F. Hou, C. Jiang, *J. Lumin.* **2006**, *116*, 67 – 72.
[23] M. Schäferling, O. S. Wolfbeis, *Chem. Eur. J.* **2007**, *13*, 4342 – 4349.
[24] S. J. Butler, D. Parker, *Chem. Soc. Rev.* **2013**, *42*, 1652 – 1666.
[25] M. L. Cable, J. P. Kirby, H. B. Gray, A. Ponce, *Acc. Chem. Res.* **2013**, *46*, 2576 – 2584.
[26] L. M. P. Lima, R. Tripier, *Curr. Inorg. Chem.* **2011**, *1*, 36 – 60.
[27] A. Heller, *J. Am. Chem. Soc.* **1966**, *88*, 2058 – 2059.
[28] D. Parker, R. S. Dickins, H. Puschmann, C. Crossland, J. A. K. Howard, *Chem. Rev.* **2002**, *102*, 1977 – 2010.
[29] C. M. Spangler, C. Spangler, M. Göttle, Y. Shen, W. J. Tang, R. Seifert, M. Schäferling, *Anal. Biochem.* **2008**, *381*, 86 – 93.
[30] Z. Lin, M. Wu, M. Schäferling, O. S. Wolfbeis, *Angew. Chem.* **2004**, *116*, 1767 – 1770; *Angew. Chem. Int. Ed.* **2004**, *43*, 1735 – 1738.
[31] N. Shao, J. Jin, G. Wang, Y. Zhang, R. Yang, J. Yuan, *Chem. Commun.* **2008**, 1127 – 1129.
[32] P. Atkinson, Y. Bretonnière, D. Parker, *Chem. Commun.* **2004**, 438 – 439.
[33] P. Atkinson, B. S. Murray, D. Parker, *Org. Biomol. Chem.* **2006**, *4*, 3166 – 3171.
[34] Y. Bretonnière, M. J. Cann, D. Parker, R. Slater, *Chem. Commun.* **2002**, 1930 – 1931.
[35] D. Parker, J. Yu, *Chem. Commun.* **2005**, 3141 – 3143.
[36] E. J. New, D. Parker, D. G. Smith, J. W. Walton, *Curr. Opin. Chem. Biol.* **2010**, *14*, 238 – 246.
[37] L. J. Charbonnière, R. Schurhammer, S. Mameri, G. Wipff, R. F. Ziessel, *Inorg. Chem.* **2005**, *44*, 7151.
[38] G. R. Choppin, *Pure Appl. Chem.* **1971**, *27*, 23 – 41.
[39] H. Takalo, E. Hänninen, J. Kankare, *Helv. Chim. Acta* **1993**, *76*, 877 – 883.
[40] I. Hyppänen, T. Soukka, J. Kankare, *J. Phys. Chem. A* **2010**, *114*, 7856 – 7867.
[41] H. Takalo, V.-M. Mukkala, H. Mikola, P. Liitti, I. Hemmilä, *Bioconjugate Chem.* **1994**, *5*, 278 – 282.
[42] R. M. Supkowski, W. DeW. Horrocks, *Inorg. Chim. Acta* **2002**, *340*, 44 – 48.
[43] A. Beeby, I. M. Clarkson, R. S. Dickins, S. Faulkner, D. Parker, L. Royle, A. S. de Sousa, J. A. G. Williams, M. Woods, *J. Chem. Soc. Perkin Trans. 2* **1999**, 493 – 593.
[44] Q. Wang, K. N. Nono, M. Syrjänpää, L. J. Charbonnière, J. Hovinen, H. Härmä, *Inorg. Chem.* **2013**, *52*, 8461 – 8466.
[45] S. L. Wu, W. DeW. Horrocks, *Anal. Chem.* **1996**, *68*, 394 – 401.
[46] N. N. Katia, A. Lecointre, M. Regueiro-Figueroa, C. Platas-Iglesias, L. J. Charbonnière, *Inorg. Chem.* **2011**, *50*, 1689 – 1697.
[47] R. Pal, D. Parker, L. C. Costello, *Org. Biomol. Chem.* **2009**, *7*, 1525 – 1528.
[48] J.-C. G. Bünzli, C. Piguet, *Chem. Soc. Rev.* **2005**, *34*, 1048 – 1077.
[49] N. M. Shavaleev, F. Gumy, R. Scopelliti, J.-C. G. Bünzli, *Inorg. Chem.* **2009**, *48*, 5611 – 5613.
[50] Sigma Quality control test procedure: Enzymatic assay of adenosine-5′-triphosphatase (EC 3.6.1.3), Sigma Prod. No. A7510.
[51] H. H. Taussky, E. Shorr, *J. Biol. Chem.* **1953**, *202*, 675 – 685.
[52] F. Ebner, *Br. J. Pharmacol.* **1990**, *101*, 337 – 343.
[53] Sigma Quality control test procedure: Enzymatic assay of apyrase (EC 3.6.1.5), ATP or ADP as substrate.
[54] P. Kadjane, M. Starck, F. Camerel, D. Hill, N. Hildebrandt, R. Ziessel, L. J. Charbonnière, *Inorg. Chem.* **2009**, *48*, 4601 – 4603.

Received: December 18, 2013
Published online on March 27, 2014